JOINT INVERSION FOR THERMAL CONDUCTIVITY AND BASAL HEAT FLUX

Susana Guzman[1] and Ruanui Nicholson[2]

[1] Department of Mathematics, The University of Auckland, Auckland 1142, New Zealand

[2] Department of Engineering Science, The University of Auckland, Auckland 1142, New Zealand

sguz318@aucklanduni.ac.nz

Keywords: *Bayesian inversion, thermal conductivity, basal heat flux, uncertainty quantification*.

ABSTRACT

In geothermal modelling, thermal data collected at the earth's surface and at well locations can help in the characterization of the subsurface. In the steady-state conductive heat flow scenario, there are two primary parameters which dictate the temperature and the heat flow distribution: the thermal conductivity within the domain of interest and the boundary conditions placed on the domain.

In the geothermal community, the problem of estimating the thermal conductivity given temperature and/or heat flow measurements is often dealt with in a deterministic framework for efficiency. Furthermore, boundary conditions are often taken to be known precisely or are calibrated manually.

Instead, we propose carrying out simultaneous inversion for both the thermal conductivity and the basal heat flux in the statistical, in particular Bayesian, framework. We show that this can be done for essentially the same computational cost as carrying out inversions in the deterministic framework. The added benefits to using the Bayesian framework are twofold: prior uncertainty in the parameters can be systematically incorporated into inversions, and the resulting uncertainty in the estimated parameters can be quantified approximately, at the cost of one matrix inversion.

We also compare the local sensitivity of temperature measurements to changes in the conductivity and the basal heat flux.

1. INTRODUCTION

In geothermal modelling, one of the key challenges and goals is to accurately characterize the earth's subsurface. Characterization can involve the estimation of (a set of) key interesting parameters of the subsurface. Such parameters could include, for instance, permeability, porosity, or thermal conductivity, see, for example Kana et al. (2015) and Georgsson (2013). In this paper, however, we concentrate mainly on characterizing the subsurface by estimating the thermal conductivity. This can be useful for locating salt bodies or gas hydrate deposits (McAliley and Li (2016)).

There has recently been a push to invert, or reverse engineer, data in the geothermal and geophysics communities to estimate parameters of interest, see for example Rath et al. (2006), Jardani and Revil (2009) and Meixner et al. (2009). Inline with this recent push we present results of inverting temperature data to calculate both the thermal conductivity and the basal heat flux term.

Recently, McAliley et al. (2016) considered a similar problem of inverting for thermal conductivity in a deterministic framework in which the basal heat flux was taken to be known exactly. We formulate the inverse problem in the Bayesian framework, which allows for systematic quantification of uncertainty in the estimated parameters of interest. We show that estimation of a representative point estimate, namely the maximum a posteriori (MAP) estimate, of the posterior density can be carried out for the effectively the same cost as carrying out inversions in the deterministic framework. Then, by taking a Gaussian approximation of the posterior, and with the additional cost of one matrix inversion we can quantify the uncertainty in the parameter (i.e. give confidence intervals for the parameter values). Related works carried out in the Bayesian framework include, among others, Wang and Beck (1989), and Rath et al. (2006).

Finally, we carry out sensitivity analysis to get a better understanding of which parameters or parts of parameters are informed by the data. Our results on the sensitivity of the data to the thermal conductivity are in line with McAliley et al. (2016), as we see fairly local resolution. i.e. the data only 'sees' the thermal conductivity near measurement points. On the other hand, our results on the sensitivity of the data to the basal heat flux indicate that the data have good resolution for the entire basal heat flux. We note that a slightly different approach to compute the sensitivities of temperature data to both thermal conductivity and basal heat flux was carried out in Ollinger et al. (2010).

The rest of the paper is set out as follows: In Section 2 we review the required theory to carry out inversions in the Bayesian framework; in Section 3 we define the forward problem and show the inversion results, discussing both the MAP estimates for both the parameters and the uncertainty in the estimates; and in Section 4 we give some concluding remarks and possible future research directions.

2. THEORY

In this section, we give the required theory to carry out inversions using the Bayesian paradigm. For an overview of the Bayesian approach to inverse problems see for example Kaipio and Somersalo (2006), Tarantola (2005) and Stuart (2010).

There are at least two key differences between the Bayesian approach and the deterministic approach to inverse problems. First, in the Bayesian framework all unknown parameters are taken to be random variables, and are assigned a prior density, or simply a prior. The prior density encodes any prior beliefs we may hold about the unknown parameters, such as constraints on possible values they may take, or the mean value they may take. Second, in the Bayesian approach the solution to the inverse problem

given as a probability density, known as the posterior density or simply the posterior.

The standard approach to constructing the posterior is by using sampling based methods such as Markov chain Monte Carlo (MCMC) methods. However, this can easily become computationally heavy or even infeasible when the number of parameters grows large due to the so-called *curse of dimensionality*. This is often the case when the parameters of interest are discretized versions of distributed parameters of partial differential equations (PDE). To avoid this problem, rather than attempting to construct the full posterior, we aim to estimate a single representative point estimate of the posterior and then approximate the posterior uncertainty. Typical choices for the representative point estimate are the conditional mean (CM) and the maximum a posteriori (MAP) estimate. The MAP estimate is typically less computationally expensive to compute than the CM estimate (Kaipio and Somersalo (2006)). We therefore only compute the MAP estimate. To approximately quantify the uncertainty in the posterior we approximate the posterior as a Gaussian density centered at the MAP and thus require the posterior covariance matrix, which can be calculated by the inversion of the Hessian matrix. The approximation of the typically non-Gaussian posterior density as Gaussian is called the Laplace approximation.

The form of the posterior depends on the forward problem, the prior density of the parameters, the density of the noise in the measurements, and the nature of that noise. In this paper we assume both the prior density and the density of the noise are Gaussian and the errors in the measurements are additive. Making these assumptions means we can write the relationship between the observed data, $\boldsymbol{d} \in \mathbb{R}^{n_d}$ and the parameters of interest $\boldsymbol{x} \in \mathbb{R}^{n_x}$ as

$$\boldsymbol{d} = \boldsymbol{f}(\boldsymbol{x}) + \boldsymbol{e}, \tag{1}$$

where $\boldsymbol{e} \sim \mathcal{N}(\boldsymbol{e}_*, \boldsymbol{\Gamma}_{\boldsymbol{e}})$ and $\boldsymbol{x} \sim \mathcal{N}(\boldsymbol{x}_*, \boldsymbol{\Gamma}_{\boldsymbol{x}})$.

Bayes' theorem states that the posterior density is proportional to the product of the likelihood and prior densities, i.e.,

$$\pi(\boldsymbol{x}|\boldsymbol{d}) \propto \pi(\boldsymbol{d}|\boldsymbol{x})\pi(\boldsymbol{x}). \tag{2}$$

It can be shown shown (e.g. in Kaipio and Somersalo (2006)) that marginalizing over the additive noise and assuming the noise is independent of the parameters of interest that the likelihood is

$$\pi(\boldsymbol{d}|\boldsymbol{x}) = \pi_{\boldsymbol{e}}(\boldsymbol{d} - \boldsymbol{f}(\boldsymbol{x})) \tag{3}$$

where $\pi_e(\cdot)$ denotes the probability density of the noise. Consequently, the posterior can be written

$$\pi(\boldsymbol{x}|\boldsymbol{d}) \propto \pi_{\boldsymbol{e}}(\boldsymbol{d} - \boldsymbol{f}(\boldsymbol{x}))\pi(\boldsymbol{x}) \tag{4}$$

$$\propto \exp\left\{-\frac{1}{2}(\| \boldsymbol{L}_{\boldsymbol{e}}(\boldsymbol{d}_{\text{obs}} - \boldsymbol{f}(\boldsymbol{x}) - \boldsymbol{e}_*) \|^2 + \| \boldsymbol{L}_{\boldsymbol{x}}(\boldsymbol{x} - \boldsymbol{x}_*) \|^2)\right\}, \tag{5}$$

where $\boldsymbol{L}_{\boldsymbol{e}}^T\boldsymbol{L}_{\boldsymbol{e}} = \boldsymbol{\Gamma}_{\boldsymbol{e}}^{-1}$, $\boldsymbol{L}_{\boldsymbol{x}}^T\boldsymbol{L}_{\boldsymbol{x}} = \boldsymbol{\Gamma}_{\boldsymbol{x}}^{-1}$, and (5) follows from (4) since $\boldsymbol{e} \sim \mathcal{N}(\boldsymbol{e}_*, \boldsymbol{\Gamma}_{\boldsymbol{e}})$ and $\boldsymbol{x} \sim \mathcal{N}(\boldsymbol{x}_*, \boldsymbol{\Gamma}_{\boldsymbol{x}})$. The MAP estimate is the parameter which maximize the posterior, i.e.

$$\boldsymbol{x}_{\text{MAP}} = arg\max_{\boldsymbol{x}\in\mathbb{R}^{n_x}} \left\{\exp\left\{-\frac{1}{2}(\| \boldsymbol{L}_{\boldsymbol{e}}(\boldsymbol{d} - \boldsymbol{f}(\boldsymbol{x}) - \boldsymbol{e}_*) \|^2 + \| \boldsymbol{L}_{\boldsymbol{x}}(\boldsymbol{x} - \boldsymbol{x}_*) \|^2)\right\}\right\} \tag{6}$$

$$= \arg\min_{\boldsymbol{x}\in\mathbb{R}^{n_x}} \left\{\frac{1}{2}(\| \boldsymbol{L}_{\boldsymbol{e}}(\boldsymbol{d} - \boldsymbol{f}(\boldsymbol{x}) - \boldsymbol{e}_*) \|^2 + \| \boldsymbol{L}_{\boldsymbol{x}}(\boldsymbol{x} - \boldsymbol{x}_*) \|^2)\right\} \tag{7}$$

Where we note that the form of (7) is also used in the deterministic framework. Computing the MAP estimate is therefore no more expensive than solving the deterministic inverse problem.

The approximate posterior covariance matrix can also be computed at the MAP estimate, as the inverse of the Gauss-Newton Hessian matrix,

$$\boldsymbol{\Gamma}_{\boldsymbol{x}|\boldsymbol{d}} = (\boldsymbol{J}_{\boldsymbol{x}}(\boldsymbol{x}_{\text{MAP}})^T\boldsymbol{\Gamma}_{\boldsymbol{e}}^{-1}\boldsymbol{J}_{\boldsymbol{x}}(\boldsymbol{x}_{\text{MAP}}) + \boldsymbol{\Gamma}_{\boldsymbol{x}}^{-1})^{-1}, \tag{8}$$

where $\boldsymbol{J}_{\boldsymbol{x}}(\boldsymbol{x}_{\text{MAP}})$ denotes the Jacobian matrix with elements $\boldsymbol{J}_{\boldsymbol{x}}(i,j) = \frac{\partial f_i}{\partial x_j}$ evaluated at $\boldsymbol{x}_{\text{MAP}}$. There is only one additional matrix inversion required to calculate $\boldsymbol{\Gamma}_{\boldsymbol{x}|\boldsymbol{d}}$ as the matrices $\boldsymbol{\Gamma}_{\boldsymbol{e}}^{-1}$ and $\boldsymbol{\Gamma}_{\boldsymbol{x}}^{-1}$ are already computed in order to find $\boldsymbol{x}_{\text{MAP}}$.

In this paper, we are interested in carrying out inversion for two parameters, namely the thermal conductivity $\boldsymbol{\sigma} \in \mathbb{R}^n$, and the basal heat flux $\boldsymbol{g} \in \mathbb{R}^m$. We suppose $\boldsymbol{\sigma} \sim \mathcal{N}(\boldsymbol{\sigma}_*, \boldsymbol{\Gamma}_{\boldsymbol{\sigma}})$ and $\boldsymbol{g} \sim \mathcal{N}(\boldsymbol{g}_*, \boldsymbol{\Gamma}_{\boldsymbol{g}})$. In this paper we treat the two parameters as independent, although there is some work suggesting they may be correlated (Ollinger et al. (2010)). We make the substitution

$$\boldsymbol{x} = \begin{pmatrix}\boldsymbol{\sigma}\\ \boldsymbol{g}\end{pmatrix},$$

so the prior of $\boldsymbol{x}$ is then

$$\boldsymbol{x} \sim \mathcal{N}\left(\begin{pmatrix}\boldsymbol{\sigma}_*\\ \boldsymbol{g}_*\end{pmatrix}, \begin{pmatrix}\boldsymbol{\Gamma}_{\boldsymbol{\sigma}} & \boldsymbol{0}\\ \boldsymbol{0} & \boldsymbol{\Gamma}_{\boldsymbol{g}}\end{pmatrix}\right), \tag{9}$$

and the MAP estimate of $\boldsymbol{x}$ is

$$\boldsymbol{x}_{\text{MAP}} = \arg\min_{\boldsymbol{x}\in\mathbb{R}^{n+m}} \left\{-\frac{1}{2}(\| \boldsymbol{L}_e(\boldsymbol{d} - \boldsymbol{f}(\boldsymbol{\sigma}, \boldsymbol{g}) - \boldsymbol{e}_*) \|^2 + \| \boldsymbol{L}_{\sigma}(\boldsymbol{\sigma} - \boldsymbol{\sigma}_*) \|^2 + \| \boldsymbol{L}_g(\boldsymbol{g} - \boldsymbol{g}_*) \|^2)\right\},$$

and the posterior covariance matrix is as in (8), with $\boldsymbol{J}_{\boldsymbol{x}} = (\boldsymbol{J}_{\boldsymbol{\sigma}}, \boldsymbol{J}_{\boldsymbol{g}})$. The posterior covariance can be expressed as

$$\boldsymbol{\Gamma}_{\boldsymbol{x}|\boldsymbol{d}} = \begin{pmatrix}\boldsymbol{\Gamma}_{\boldsymbol{\sigma}|\boldsymbol{d}} & \boldsymbol{\Gamma}_{\boldsymbol{\sigma}\boldsymbol{g}|\boldsymbol{d}}\\ \boldsymbol{\Gamma}_{\boldsymbol{g}\boldsymbol{\sigma}|\boldsymbol{d}} & \boldsymbol{\Gamma}_{\boldsymbol{g}|\boldsymbol{d}}\end{pmatrix}.$$

3. NUMERICAL EXAMPLE

In this section, we outline the numerical aspects of the forward and inverse problems, and discuss the results of the inversion. To assess the usefulness of the measurements with respect to both the conductivity and basal heat flux we also carry out local sensitivity analysis.

The forward problem is the mapping from the parameters of interest to the measured data. The parameters of interest (which we wish to invert for) in this paper are both the isotropic thermal conductivity $\boldsymbol{\sigma}$ and the basal flux $\boldsymbol{g}$ in the domain Ω.

3.1 Forward Problem

We take our domain of interest, Ω, to be a two-dimensional slice of the earth's subsurface. Assuming that the temperature distribution within Ω does not evolve in time, the temperature within Ω is governed by the steady-state heat equation.

We impose no heat flux on the left and right hand sides of the domain. On the top side of the domain, we impose a radiation type boundary condition in an attempt to account for heat transferred between the air and the ground, while on the bottom side of the domain, we stipulate positive heat flux. The mapping from the parameters of interest to the temperature throughout the domain in this case is given by the solution to the following steady-state heat equation:

$$\begin{aligned} -\nabla\cdot(\exp(\sigma)\nabla u) &= 0 && in\ \Omega \\ \exp(\sigma)\nabla u\cdot\boldsymbol{n} &= 0 && on\ \Gamma_{\mathrm{s}} \\ \exp(\sigma)\nabla u\cdot\boldsymbol{n}+\beta u &= 0 && on\ \Gamma_{\mathrm{t}} \\ \exp(\sigma)\nabla u\cdot\boldsymbol{n} &= \exp(g) && on\ \Gamma_{\mathrm{b}}. \end{aligned} \tag{10}$$

Here u is the temperature, σ denotes thermal conductivity, and g represents the basal heat flux. The "exp" function is used to ensure positivity of both thermal conductivity and basal heat flux. It is therefore technically the log thermal conductivity and log basal heat flux which we invert for. For simplicity, we assume the ambient temperature of the air at the topside of the domain is zero. We note that it may be possible to invert for the parameter β, but in this paper we set $\beta = 1$.

The domain of interest is taken to be the rectangle $\Omega = [0,1]\times[0,0.2]$ for simplicity. To solve the forward problem we use the finite element method (FEM) with 2,000 piece-wise linear basis functions over 3,762 triangular elements. The mesh is shown on the left in Figure 1.

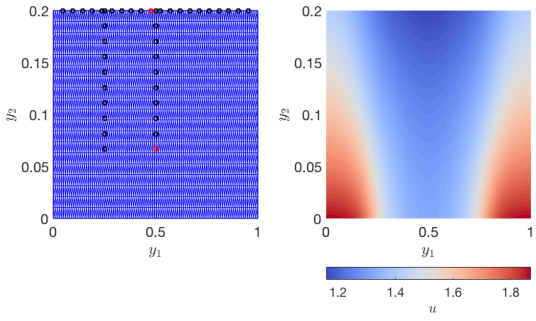

Figure 1: The mesh, the measurements and the temperature. Left: The mesh used for the inversions as well as the measurement locations as circles (red circles show where sensitivity analysis is carried out). Right: The true temperature distribution from which measurements are taken.

Measurements used for the inversion are 40 point-wise temperature measurements at points along Γ_{t} as well as at well locations within Ω. Measurement locations can be seen on the left in Figure 1. Noiseless data is generated by computing $\boldsymbol{\mathcal{B}u}$, where $\boldsymbol{u}$ is the discretised FEM solution to (10) and $\boldsymbol{\mathcal{B}}$ is the linear observation operator, extracting $\boldsymbol{u}$ at the measurement locations. The temperature $\boldsymbol{u}$ corresponding to the true values of both $\boldsymbol{\sigma}$ and $\boldsymbol{g}$ throughout the domain is shown on the right of Figure 1.

3.2 Inverse Problem

Before carrying out the inversions we specify both the noise and prior densities. We take both as Gaussian. We take the noise to be zero mean white noise, i.e. $\boldsymbol{e}\sim\mathcal{N}(\boldsymbol{0},\delta_{\boldsymbol{e}}\boldsymbol{I})$. The noise level $\delta_{\boldsymbol{e}}$ is chosen as $\delta_{\boldsymbol{e}} = 1/100\times(\max\{\boldsymbol{\mathcal{B}u}\}-\min\{\boldsymbol{\mathcal{B}u}\})$ i.e. the noise level is 1% of the range of the noiseless measurements.

We now specify the prior densities on $\boldsymbol{\sigma}$ and $\boldsymbol{g}$. For simplicity we take $\boldsymbol{\sigma}_* = \boldsymbol{0}$ and $\boldsymbol{g}_* = \boldsymbol{0}$. The prior covariance matrices are taken by first considering the PDE operators

$$\overline{\boldsymbol{L}}_\sigma = \alpha_\sigma\boldsymbol{K}+\gamma_\sigma\boldsymbol{M} \qquad \overline{\boldsymbol{L}}_g = \alpha_g\boldsymbol{\mathcal{K}}+\gamma_g\boldsymbol{\mathcal{M}}$$

where $\boldsymbol{K}_{ij} = \int_\Omega \boldsymbol{\Theta}_\sigma\nabla\phi_i\cdot\nabla\phi_j\,d\boldsymbol{y}$ and $\boldsymbol{\mathcal{K}}_{ij} = \int_{\Gamma_{\mathrm{b}}}\nabla\phi_i\cdot\nabla\phi_j\,ds$ are stiffness matrices, $\boldsymbol{M}_{ij} = \int_\Omega\phi_i\phi_j\,d\boldsymbol{y}$ and $\boldsymbol{\mathcal{M}}_{ij} = \int_{\Gamma_{\mathrm{b}}}\phi_i\phi_j\,ds$ are mass matrices, $\alpha_\sigma,\alpha_g,\gamma_\sigma,\gamma_g>0$ control the respective variances, and $\boldsymbol{\Theta}_\sigma$ is a symmetric positive definite matrix which determines the correlation structure of $\boldsymbol{\sigma}$. Then inline with Lindgren et al. (2011) we take $\overline{\boldsymbol{\Gamma}}_\sigma = \overline{\boldsymbol{L}}_\sigma\boldsymbol{M}^{-1}\overline{\boldsymbol{L}}_\sigma$ and $\overline{\boldsymbol{\Gamma}}_g = \overline{\boldsymbol{L}}_g\boldsymbol{\mathcal{M}}^{-1}\overline{\boldsymbol{L}}_g$ and take

$$\boldsymbol{\Gamma}_\sigma = \delta_\sigma^2\boldsymbol{W}\overline{\boldsymbol{\Gamma}}_\sigma\boldsymbol{W}^T,$$

$$\boldsymbol{\Gamma}_g = \delta_g^2\boldsymbol{\mathcal{W}}\overline{\boldsymbol{\Gamma}}_g\boldsymbol{\mathcal{W}}^T,$$

where $\boldsymbol{W}$ and $\boldsymbol{\mathcal{W}}$ are diagonal matrices such that $\mathrm{diag}(\boldsymbol{W}) = \mathrm{diag}(\overline{\boldsymbol{\Gamma}}_\sigma)^{-\frac{1}{2}}$ and $\mathrm{diag}(\boldsymbol{\mathcal{W}}) = \mathrm{diag}(\overline{\boldsymbol{\Gamma}}_g)^{-1/2}$. In the current setting, the inverse problem consists of two parts:

1. Finding the MAP estimate for the thermal conductivity and basal heat flux, $\boldsymbol{x}_{\mathrm{MAP}}$, given the temperature measurements.

2. Approximately quantifying the posterior uncertainty by calculating the posterior covariance matrix $\boldsymbol{\Gamma}_{\boldsymbol{x}|\boldsymbol{d}}$ at the MAP estimate.

Finding the MAP estimate equates to solving the minimization problem of (7). Minimization is carried out using the Gauss-Newton method, initialised at the prior means. To avoid the computational burden of calculating the Jacobian matrix using finite differencing, we use an adjoint approach. Once the search direction is found we use MATLAB's built in *fminsearch* function with an initial step length of 1 to carry out the line search. Convergence is established once the norm of the gradient of the cost function is reduce by a factor of 10^5.

Computing the posterior covariance matrix amounts to inverting a matrix, see formula (8). We note that in the high dimensional case i.e. $\boldsymbol{\sigma}\in\mathbb{R}^n$ and $\boldsymbol{g}\in\mathbb{R}^m$ with n and/or m very large (of order 10^5 for example), that direct inversion may be computationally infeasible. In such cases, a low rank approximation of $\boldsymbol{\Gamma}_{\boldsymbol{x}|\boldsymbol{d}}$ may need to be employed Bui-Thanh, et al. (2013).

3.3 Inversion and uncertainty results

Here we examine the estimates from the inverse problem. We simultaneously discuss the calculated MAP estimates and the approximated posterior covariance.

On the left of Figure 2 we show the true thermal conductivity used to generate the synthetic measurements, and on the right we show the reconstructed MAP estimate. The estimate is qualitatively and quantitatively in good agreement with the truth, although the values are slightly overestimated throughout the domain. The point-wise standard deviation is shown on the right of Figure 3. We conclude that the true conductivity is well contained in the estimated posterior density as the true conductivity is generally within 3 posterior standard deviations of the estimate.

The prior standard deviation is shown on the left of Figure 3. It is clear that the approximate posterior standard deviation is (in some places substantially) less than the prior standard deviation, i.e. by taking into account the measurements we can reduce the uncertainty in the thermal conductivity.

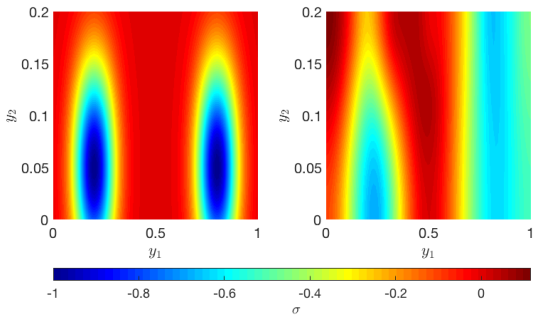

Figure 2: The estimate for conductivity $\boldsymbol{\sigma}$. Left: The true thermal conductivity $\boldsymbol{\sigma_{\text{true}}}$. Right: The MAP estimate for the thermal conductivity $\boldsymbol{\sigma_{\text{MAP}}}$.

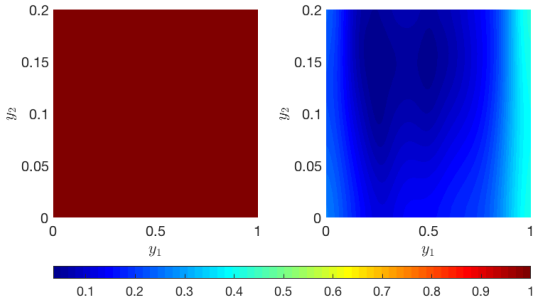

Figure 3: The variance in $\boldsymbol{\sigma}$. Left: The prior standard deviation of $\boldsymbol{\sigma}$. Right: The approximate posterior variance of $\boldsymbol{\sigma}$.

On the left of Figure 4 we show the prior mean and covariance for the basal heat flux, while on the right we show the MAP estimate, the posterior confidence intervals and the true basal heat flux. We see good agreement between the MAP estimate and the true value of the basal heat flux. Interestingly the posterior variance is only slightly less than the prior variance along most of the basal boundary.

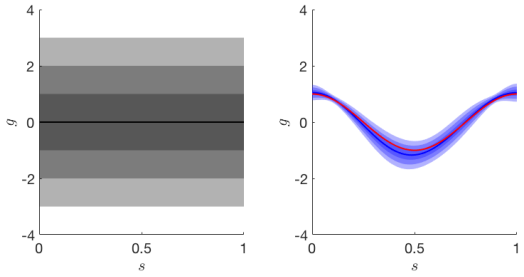

Figure 4: The estimate for $\boldsymbol{g}$. Left: The initial guess, which is also the prior mean for the basal heat flux, $\boldsymbol{g_*}$, along with the ± 3 prior standard deviation intervals. Right: The MAP estimate for the basal heat flux, $\boldsymbol{g_{\text{MAP}}}$ (blue line), along with ± 3 approximate posterior standard deviation intervals ad true basal heat flux, $\boldsymbol{g_{\text{true}}}$ (red line).

3.4 Local sensitivity analysis

To determine how "useful" each of the measurements are, we carry out localised sensitivity analysis at the prior mean. The sensitivity of the *i*-th measurement, $f_i(\boldsymbol{x})$, to the *j*-th parameter, x_j evaluated at $\boldsymbol{x} = \boldsymbol{x}_*$ is given by

$$\frac{\partial f_i(\boldsymbol{x})}{\partial x_j}|_{\boldsymbol{x}=\boldsymbol{x}_*},$$

which is the ij^{th} element of the Jacobian matrix (sensitivity matrix) evaluated at $\boldsymbol{x} = \boldsymbol{x}_*$. We investigate the sensitivities of two different measurements to both the conductivity and basal heat flux.

The two measurement locations are chosen a) at a measurement location near the centre on the top of the domain (the 20^{th} measurement point), and b) at the bottom measurement location of the right hand well (the 21^{st} measurement point), see Figure 1 for the exact location of these measurement points.

The sensitivities for the 20^{th} and 21^{st} measurements are shown in Figures 5 and 6 respectively. In each figure, sensitivities with respect to $\boldsymbol{\sigma}$ are shown on the left, while sensitivities with respect to $\boldsymbol{g}$ are shown on the right. Inline with McAliley and Li (2016) we see that the sensitivities with respect to $\boldsymbol{\sigma}$ are fairly localised i.e. the data is only influenced by nearby values of $\boldsymbol{\sigma}$. On the other hand, the sensitivities with respect to $\boldsymbol{g}$ are fairly widespread i.e. the data is influenced by values of $\boldsymbol{g}$ at practically any point of the domain.

4. CONCLUSION

In this paper, we considered the two dimensional inverse problem of estimating both the thermal conductivity and the basal heat flux from temperature measurements taken on the top of the domain and at well locations throughout the domain. The inverse problem was posed in the Bayesian framework so as to allow for straight forward quantification of the posterior uncertainty in the parameters.

We showed that to calculate the MAP estimate requires essentially the same computational cost as to carry out deterministic inversions. Furthermore with the additional cost of one matrix inversion the approximate uncertainty in the parameters could be computed.

Finally, we briefly looked at the sensitivity of the data to the two parameters. This sensitivity analysis showed that the sensitivity of the data to the thermal conductivity was fairly localised whereas for the basal heat flux the sensitivity was widespread across the bottom boundary.

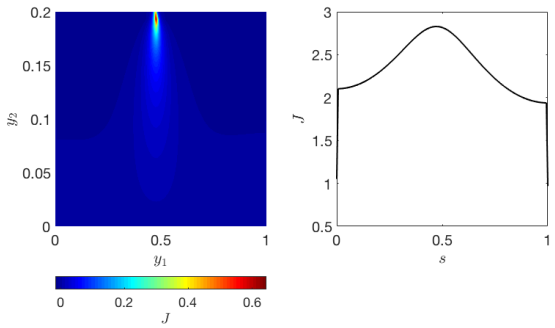

Figure 5: Local sensitivity analysis for measurement location 20. Left: The sensitivity of the 20^{th} measurement point to the conductivity, σ throughout the domain. Right: The sensitivity of the 20^{th} measurement point to the basal heat flux g along the bottom of the domain.

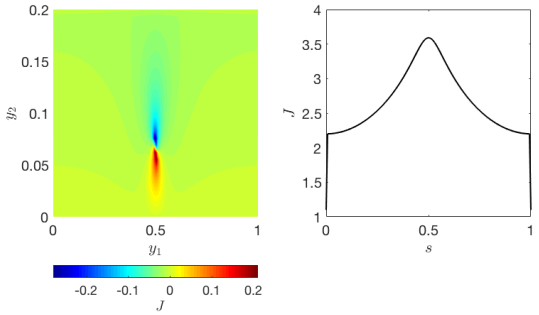

Figure 6: Local sensitivity analysis for measurement location 21. Left: The sensitivity of the 21^{st} measurement point to the conductivity, σ throughout the domain. Right: The sensitivity of the 21^{st} measurement point to the basal heat flux g along the bottom of the domain.

ACKNOWLEDGEMENTS

We acknowledge Jari Kaipio and Owen Dillon for valuable input to this paper.

REFERENCES

Bui-Thanh, Tan, et al. "A computational framework for infinite-dimensional Bayesian inverse problems Part I: The linearized case, with application to global seismic inversion." SIAM Journal on Scientific Computing 35.6 (2013): A2494-A2523.

Georgsson, Lúðvík S. "Geophysical methods used in geothermal exploration." (2013).

Jardani, A., and A. Revil. "Stochastic joint inversion of temperature and self-potential data." Geophysical Journal International 179.1 (2009): 640-654.

Jokinen, Jarkko, and Ilmo T. Kukkonen. "Inverse simulation of the lithospheric thermal regime using the Monte Carlo method." Tectonophysics 306.3-4 (1999): 293-310.

Kaipio, Jari, and Erkki Somersalo. Statistical and computational inverse problems. Vol. 160. Springer Science & Business Media, 2006.

Kana, Janvier Domra, et al. "A review of geophysical methods for geothermal exploration." Renewable and Sustainable Energy Reviews 44 (2015): 87-95.

Lindgren, Finn, Håvard Rue, and Johan Lindström. "An explicit link between Gaussian fields and Gaussian Markov random fields: the stochastic partial differential equation approach." Journal of the Royal Statistical Society: Series B (Statistical Methodology) 73.4 (2011): 423-498.

McAliley, Andy, and Yaoguo Li "3D inversion of heat flow data for thermal conductivity." *SEG Technical Program Expanded Abstracts 2016*. Society of Exploration Geophysicists, 2016. 1553-1557.

Meixner, Tony, et al. "Stochastic temperature, heat flow and geothermal gradient modeling direct from a 3D map of the Cooper Basin region, Central Australia." *SEG Technical Program Expanded Abstracts 2010*. Society of Exploration Geophysicists, 2010. 1100-1106.

Ollinger, Dieter, et al. "Distribution of thermal conductivities in the Groß Schönebeck (Germany) test site based on 3D inversion of deep borehole data." *Geothermics* 39.1 (2010): 46-58.

Rath, V., A. Wolf, and H. M. Bücker. "Joint three-dimensional inversion of coupled groundwater flow and heat transfer based on automatic differentiation: sensitivity calculation, verification, and synthetic examples." *Geophysical Journal International* 167.1 (2006): 453-466.

Revil, A., and Nicolas Florsch. "Determination of permeability from spectral induced polarization in granular media." *Geophysical Journal International* 181.3 (2010): 1480-1498.

Stuart, Andrew M. "Inverse problems: a Bayesian perspective." *Acta Numerica* 19 (2010): 451-559.

Tarantola, Albert. *Inverse problem theory and methods for model parameter estimation*. Vol. 89. siam, 2005.

Wang, K., and A. E. Beck. "An inverse approach to heat flow study in hydrologically active areas." *Geophysical Journal International* 98.1 (1989): 69-84.